

# SEARCHES FOR BEYOND SM HIGGS BOSON AT THE TEVATRON

A. Safonov

(for CDF and D0 Collaborations)

*Department of Physics, Texas A&M University, 4242 TAMU,  
College Station, TX 77843, USA*

In the following, we describe preliminary results of searches for non-SM higgs bosons at the CDF and D0 experiments. Both experiments use data obtained in  $p\bar{p}$  collisions at the Tevatron at  $\sqrt{s} = 1.96$  TeV.

## 1 Introduction

The Higgs mechanism is the heart of the Standard Model (SM) providing masses to gauge bosons via electroweak symmetry breaking (EWSB). However, the SM fails to explain the origin of the Higgs mechanism and has certain naturalness problems, such as the extreme fine tuning required to keep the higher order corrections to the higgs mass under control (the so called hierarchy problem). In popular SM extensions, such as minimal SUSY (MSSM)<sup>1</sup> and Little(st) Higgs<sup>2</sup> models, the EWSB is radiatively generated and these models are free from many of the above difficulties. In these models, the higgs sector is typically more complex, requiring additional neutral and charged higgs bosons in MSSM, and even doubly charged higgs bosons in Little Higgs, SUSY with extended higgs sector, and Left-Right symmetric<sup>3</sup> models. While the production cross section of higgs bosons is usually model dependent, the phenomenology in terms of decay modes and production mechanisms are often similar for a wide variety of new phenomena scenarios. This simplifies the interpretation of the experimental results: while the cross section driven mass limits are usually model dependent, production cross section limits obtained for certain benchmark scenarios are often applicable to other models.

## 2 Neutral Higgs Boson Searches

Apart from the SM, neutral higgs bosons appear in almost every scenario exploring new phenomena. A typical example is the MSSM, where the higgs sector consists of three neutral higgs bosons: two scalars,  $h$  and  $H$ , and a pseudoscalar  $A$  (and also two charged higgs fields  $H^\pm$ ). Compared to SM, there are differences in higgs production mechanisms. In MSSM at large  $\tan\beta$  there is a strong enhancement of the cross-section for the dominant production channel  $gg \rightarrow \phi$  ( $\phi = A$  and  $h$  or  $H$ ) due to additional diagrams with a  $b$ -quark in the loop. The cross-section in this case scales as  $\tan^2\beta$ . Similarly, there is a strong enhancement of diagrams with  $b$ -quarks in the final state coming from the proton/antiproton sea or from radiative pair production leading to additional experimental signatures of higgs produced in association with one or two  $b$ -jets.

For the majority of the MSSM parameter space, light higgs bosons decay predominantly to  $b\bar{b}$  ( $Br \simeq 90\%$ ) and  $\tau\tau$  ( $Br \simeq 8-9\%$ ). However, one should note that the radiative corrections may

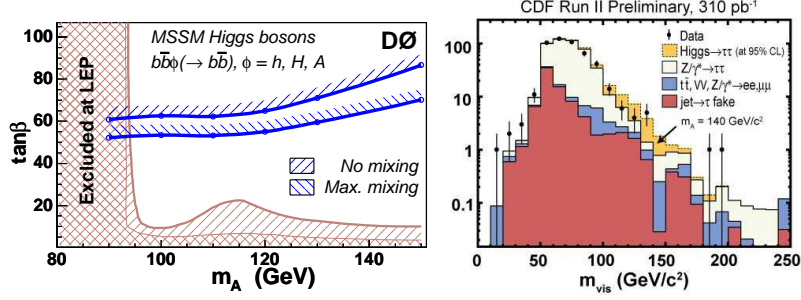


Figure 1: Left: The exclusion plot in the MSSM  $m_A$  versus  $\tan\beta$  plane for  $h b\bar{b} \rightarrow b\bar{b} b\bar{b}$  search. Right: Invariant mass of lepton, tau and  $\cancel{E}_T$  in the  $h \rightarrow \tau\tau$  analysis.

violate the fermion mass universality of the higgs coupling and lead to a strong suppression of the higgs coupling to  $b$ -quarks making taus the best bet for discovering MSSM higgs. Experimentally, the use of the  $b\bar{b}$  decay modes is most effective for processes involving additional objects (e.g.  $b$ -jets). Just as in the SM case, the very high cross section of QCD  $b\bar{b}$  production at  $p\bar{p}$  colliders precludes one from using the dominant  $gg \rightarrow h/A/H$  mode. This loss can be partially recovered by using the  $\tau\tau$  final state that has a much cleaner signature, but suffers from the lower branching ratio compared to  $b$ -jets.

### 2.1 Search for $Hb(b) \rightarrow b\bar{b}b(b)$

This D0 analysis<sup>4</sup> searches for MSSM higgs bosons at large  $\tan\beta$  decaying to a pair of  $b$ -jets and produced in association with one or more additional  $b$ -jets using 260 pb<sup>-1</sup> of data. Events are required to have at least three jets in the  $|\eta| < 2.5$  region passing thresholds of 35, 20 and 15 GeV and tagged as  $b$ -jets using the Secondary Vertex (SV) tagging algorithm. The SV tagging efficiency is about 55% for central  $b$ -jets with  $E_T > 35$  GeV, while the rate of light quark jets being misidentified as  $b$ -jets is  $\simeq 1\%$ . The two highest  $E_T$  jets are used to form an invariant mass, which is used as the final discriminating variable between signal and SM backgrounds. Shape of the backgrounds due to mistags is estimated using a data sample selected similar to the signal case except that only two jets have to be tagged as  $b$ -jets (rather than three), and where the  $E_T$  dependent mistag rates are applied to the non-tagged jets. Simulation shows that the remaining background contributions from  $b\bar{b}b\bar{b}$  and  $Zb\bar{b} \rightarrow b\bar{b}b\bar{b}$  have shapes similar to that of the mistag sample. Data selected in the signal region is then fitted using shapes of the signal and backgrounds (taken from the mistag sample) for the normalization of a possible higgs signal. Signal acceptance is obtained using Pythia; production cross section and branching ratios come from the CPsuperH program. With no deviation from SM, the analysis sets a limit on the production cross section of MSSM higgs in this topology. The cross section limit is then re-interpreted in terms of the MSSM parameters  $\tan\beta$  and  $m_A$  (mass of the pseudoscalar). Results are presented in Fig. 1, lines show the part of the parameter space excluded at 95% C.L.

### 2.2 Search for $H \rightarrow \tau\tau$

Both CDF and D0 perform a search for higgs decaying to a pair of tau leptons. The CDF analysis<sup>5</sup> uses 320 pb<sup>-1</sup> and relies on the data selected using lepton+track triggers. The offline selections require a reconstructed light lepton ( $e$  or  $\mu$ ) with transverse energy of 10 GeV and a hadronically decaying tau candidate with  $p_T > 15$  GeV/ $c$ . To suppress backgrounds due to QCD jet production, an additional requirement  $p_T^\tau + p_T^l + \cancel{E}_T > 50$  GeV ( $\cancel{E}_T$  is missing transverse energy) is applied. Final events are used to construct an invariant mass of lepton, tau, and  $\cancel{E}_T$ , and the distribution is fitted for a combination of possible signal and SM background (see Fig. 1.

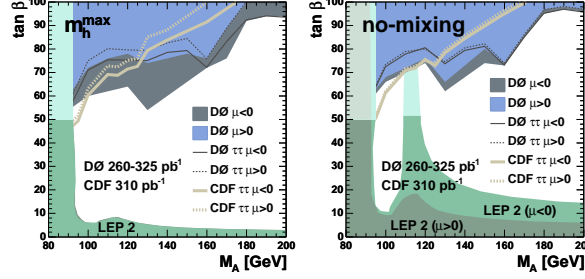


Figure 2: The exclusion plot in the MSSM  $m_A$  versus  $\tan\beta$  plane for  $H \rightarrow \tau\tau$  search for  $m_h^{max}$  (left) and no mixing (right) scenarios showing both CDF and the combined D0  $H \rightarrow \tau\tau$  and  $Hb(b) \rightarrow bbb(b)$  results.

With no excess found in the data CDF sets a limit on MSSM higgs production cross section, which is then re-interpreted in terms of an exclusion plot in the  $\tan\beta$  versus  $m_A$  plane shown in Fig. 2.

The D0  $H \rightarrow \tau\tau$  analysis is based on  $350 \text{ pb}^{-1}$  of data collected using inclusive electron and muon triggers as well as an  $e + \mu$  trigger. Light leptons are required to pass  $p_T > 14 \text{ GeV}/c$ . A neural net technique is used to select hadronically decaying tau candidates with  $p_T > 20 \text{ GeV}/c$ . The neural net is separately optimized for  $\pi$ ,  $\rho$  and “3-prong”-like hadronic tau topologies and the main variables allowing discrimination against QCD jets are related to isolation and differences in shower profile. After additional topological cuts to suppress backgrounds from multi-jet and  $W$ +jet production, the distribution of the invariant mass of lepton, tau, and  $\cancel{E}_T$  (or two leptons and  $\cancel{E}_T$  for the  $e\mu$  channel) is fitted for a combination of possible higgs signal and SM backgrounds. With no evidence of the new physics signal, a 95% C.L. limit on the maximum allowed cross section is set. The obtained limit is then interpreted as an exclusion region in the plane of  $\tan\beta$  versus  $m_A$  for the same benchmark points as in the CDF analysis using the FEYNHIGGS program. Figure 2 shows the combined limit from this analysis and the one in the  $Hb(\bar{b}) \rightarrow b\bar{b}b(\bar{b})$  channel.

### 3 Charged Higgs Searches

The charged higgs is predicted in the MSSM and appears in other beyond-SM scenarios with expanded higgs sector. In the MSSM, direct production of  $H^\pm$  at the Tevatron is negligible, however, charged higgs bosons can be produced in top quark decays, predominantly via  $t \rightarrow bH^\pm$ . This new decay mode will modify the branching ratios for the top quark decay modes, i.e. lower fraction of  $t \rightarrow Wb$ . In turn, the  $H^\pm$  decay modes are different from those of  $W$  bosons: MSSM  $H^+$  branching ratios are a strong function of  $\tan\beta$ , but at high  $\tan\beta$   $H^+$  preferably decays into  $\tau\nu$ , while  $W$  leptonic decay modes are nearly democratic among generations). Therefore, one can detect the presence of  $H^\pm$  by observing a violation of the top branching ratios prescribed by the SM. This search<sup>6</sup> uses  $192 \text{ pb}^{-1}$  of CDF data and analyzes the following top samples: (i) dilepton ( $e$  or  $\mu$ ) plus jets; (ii) lepton+jets with exactly one  $b$ -tag; (iii) lepton+jets with exactly two or more  $b$ -tags; and (iv) lepton+hadronic tau with two or more jets. Signals of new physics will lead to a deviation of the observed number of events in these samples compared to the SM prediction. The data is selected using standard selections with lepton and tau  $p_T > 20 \text{ GeV}/c$  and the  $b$ -jets are tagged using a secondary vertex algorithm. The number of expected(observed) events in each of the four categories above is 11(13), 54(49), 10(8) and 2(2). With no disagreement, a limit is set on the production cross-section. Using MSSM as a reference model, the results are interpreted as an exclusion region in the  $m_{H^\pm}$  versus  $\tan\beta$  plane for several benchmark points. Figure 3 shows the excluded region for one of the selected points.

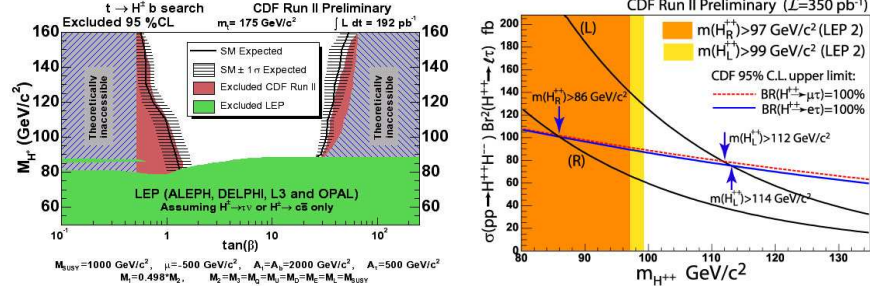


Figure 3: Left: Exclusion plot in the MSSM  $m_{H^\pm}$  versus  $\tan\beta$  plane for charged higgs search. Right: 95% C.L. upper limit on the production cross section of doubly charged higgs boson predicted by Left-Right symmetric models.

#### 4 Doubly Charged Higgs Searches

The doubly charged higgs  $H^{++}$  appears in the Left-Right symmetric models, SUSY, and Little Higgs models. At the Tevatron, the main production mechanism for doubly charged higgs is pair production. Decay modes to leptons are largely unrestricted including possible lepton flavor violation (LFV), while decays to  $W$ 's are suppressed by the  $\rho$  parameter. CDF has published a paper<sup>7</sup> on a search for pair produced doubly charged higgs bosons decaying to  $ee$ ,  $e\mu$  and  $\mu\mu$  in the context of a LR-symmetric model<sup>3</sup> strengthening previous limits from LEP. The current analysis searches for  $H^{++} \rightarrow e\tau$  and  $\mu\tau$ , two out of the three remaining modes (the other one is  $\tau\tau$ ). LEP data excludes  $H^{++}$  of these kinds for  $m_H > 97 - 99 \text{ GeV}/c^2$ .

Analysis starts by requiring an electron or muon candidate with  $p_T > 20 \text{ GeV}/c$  and a hadronic tau with  $p_T > 15 \text{ GeV}/c$ . At least one additional “isolated track system” (ITS) is required (in  $e + \tau$  analysis this system has to additionally match a calorimeter cluster). All passing events are divided into 3- and 4-particle categories:  $l + \tau + ITS$  and  $l + \tau + ITS + ITS$ . A set of event topology cuts are applied to suppress remaining backgrounds in events of the 3-particle topology (4-particle events are already very clean). The choice of the event topology cuts is optimized for each of the two categories individually to maximize significance. After all cuts, the expected number of events from SM backgrounds is a fraction of an event in each category and no events in data are found. With no excess, the analysis sets a limit on LFV  $H^{++}$  species in these channels, as shown in Fig. 3.

#### Acknowledgments

The author would like to thank the US National Science Foundation for providing partial funding support (Award No.: PHY-0611671).

#### References

1. D.J.H. Chung *et al.*, *Phys. Rept.* **407**, 1 (2005) and references therein.
2. N. Arkani-Hamed, A. G. Cohen and H. Georgi, *Phys. Lett. B* **513**, 232 (2001).
3. R. N. Mohapatra and J. C. Pati, *Phys. Rev. D* **11**, 566 (1975).
4. V. Abazov *et al.* (D0 Collaboration), *Phys. Rev. Lett.* **95**, 151801 (2005).
5. A. Abulencia *et al.* (CDF Collaboration), Submitted to *Phys. Rev. Lett.*, hep-ex/0508051.
6. A. Abulencia *et al.* (CDF Collaboration), Submitted to *Phys. Rev. Lett.*, hep-ex/0510065.
7. D. Acosta *et al.* (CDF Collaboration), *Phys. Rev. Lett.* **93**, 221802 (2004).